Primary-Consistent Soft-Decision Color Demosaicking for Digital Cameras (Patent Pending)

Xiaolin Wu, *Senior Member, IEEE,* and Ning Zhang

***Abstract*—Color mosaic sampling schemes are widely used in digital cameras. Given the resolution of CCD sensor arrays, the image quality of digital cameras using mosaic sampling largely depends on the performance of the color demosaicking process. A common problem with existing color demosaicking algorithms is an inconsistency of sample interpolations in different primary color channels, which is the cause of the most objectionable color artifacts. To cure the problem, we propose a new primary-consistent soft-decision framework (PCSD) of color demosaicking. In the PCSD framework, we make multiple estimates of a missing color sample under different hypotheses on edge or texture directions. The estimates are made via a primary consistent interpolation, meaning that all three primary components of a color are interpolated in the same direction. The final estimate of a color sample is obtained by testing different interpolation hypotheses in the reconstructed full-resolution color image and selecting the best via an optimal statistical decision or inference process. A concrete color demosaicking method of the PCSD framework is presented. This new method eliminates certain types of color artifacts of existing color demosaicking methods. Extensive experimental results demonstrate that the PCSD approach can significantly improve the image quality of digital cameras in both subjective and objective measures. In some instances, our gain over the competing methods can be as much as 7 dB.**

***Index Terms*—Bayer CCD pattern, color demosaicking, digital cameras, Fisher discriminant, second-order Laplacian correction filter, soft decision.**

I. Introduction

THE COLOR mosaic CCD sensor arrays like the well-known Bayer pattern [3] are widely used in digital cameras because of their simplicity and low cost. However, an inherent drawback of the color mosaic is the subsampling of primary colors, particularly in red and blue channels. Color demosaicking via adaptive and robust sample interpolation thus holds the key to the visual quality of digital cameras. Many color demosaicking algorithms were proposed [1]–[5], [8]–[10]. For an up-to-date comprehensive literature survey on color demosaicking for digital cameras, we refer the reader to the introduction part of a recent paper of Gunturk *et al.* [8], and to a good website on the topic [5]. Also, an excellent informative introduction to color demosaicking among other technical problems of digital cameras can be found in [2] by Adams *et al.* Central to the color demosaicking process is gradient-guided directional interpolation. The main idea is to reconstruct the missing samples via interpolation along rather than across the edges. However, many existing color demosaicking algorithms suffer from an inadvertent oversight of not imposing the consistency of interpolation directions in three primary colors red, green, and blue, despite their efforts to exploit the correlation between the color channels. Fine objects in a scene such as hairs and cloth threads, which the existing color demosaicking algorithms often fail to reconstruct, typically have a constant hue and subtle changes, if any, in intensity and/or saturation due to illumination conditions. Consequently, there is a high degree of agreement in the gradients of the three primary colors in natural images, which we call primary consistency. This is an important physical constraint. The violation of this consistency causes objectionable visual artifacts. A main contribution of this paper is the new concept of primary-consistent color interpolation. Although the ubiquitous (R, G, B) Bayer color mosaic pattern is assumed throughout the paper, the term color primaries in the discussions hereafter should be understood more generally to include individual color components in other color spaces such as (Y, Cr, Cb), (X, Y, Z), etc., and they can also be generalized to include individual color components if a color is represented by more than three components such as the (R, G, B, E) of the recently released Sony's new CCD, where E stands for emerald.

Another drawback of the existing color demosaicking algorithms is that they interpolate missing color components at a pixel independently of the color interpolations at neighboring pixels. The interpolation decision is made on a hypothesis of the local gradient direction. However, these algorithms do not validate the underlying hypothesis after the color interpolation is completed. The verification of the hypothesis is difficult if the pixels are treated individually. To overcome this drawback, we introduce a new notion of soft-decision color demosaic. At each pixel, instead of forcing a decision on the interpolation direction with insufficient data, we make multiple hypotheses and interpolate missing color components for each of the hypotheses. Then, we examine the interpolation results under different hypotheses in a local window, and choose the one whose underlying hypothesis agrees with the reconstructed color image the best. In other words, the decision to choose the optimal interpolation is delayed until the final color reconstruction under different hypotheses can be compared. In practice, only two hypotheses, one for horizontal structure and

Manuscript received June 16, 2003; revised December 8, 2003. This work was supported in part by the Natural Sciences and Engineering Research Council of Canada. The associate editor coordinating the review of this manuscript and approving it for publication was Dr. Zhigang (Zeke) Fan.

The authors are with the Department of Electrical and Computer Engineering, McMaster University, Hamilton, ON L8S 4K1, Canada (e-mail: xwu@mail.ece.mcmaster.ca; nzhang2@cogeco.ca).

Digital Object Identifier 10.1109/TIP.2004.832920

the other for vertical structure, suffice to eliminate most of color artifacts of the existing color demosaicking algorithms.

The new approach of interpolating missing primary color components of a pixel in a consistent direction and determining the interpolation direction via soft decision is called primary-consistent soft-decision (PCSD) demosaic. In the next section, we present a primary consistent color interpolation scheme. The consistency of interpolation direction in different color channels is not always easy to achieve in certain configurations of a local mosaic pattern. The remedy is to first interpolate missing green samples separately in multiple directions, i.e., making multiple estimates under different hypotheses on edge directions. Then, the interpolations of missing red and blue samples are carried out also separately under each of the hypotheses and aided by the corresponding directional green estimates. In Section III, we complete the development of the PCSD framework by introducing the concept of soft-decision color demosaicking in choosing the primary-consistent estimates under different hypotheses. A concrete realization of the PCSD framework is proposed that uses Fisher's linear discriminant to make an optimal decision between two estimates under horizontal and vertical edge hypotheses. Section IV presents experimental results of the proposed PCSD-based method. It also offers a comparison study between the new color demosaicking method and the existing ones. In order to not interrupt the presentation flow, some relatively lengthy detailed analyzes of the problems associated with inconsistency of interpolation directions and with hard decision in color demosaicking are presented in Appendices A and B.

II. Primary-Consistent Color Interpolation

A natural tendency in designing a gradient-guided color demosaicking algorithm is to estimate the gradient at the highest directional resolution possible. Two cases in point are rather elaborated methods of directional interpolation proposed by Chang *et al.* [4] and Adams *et al.* [1]. These methods differentiate sample values in all eight digital directions and reconstruct the missing color component by selecting and weighing one or more directional interpolations along a probable edge. Surprisingly, though, the end effects of such methods, in some cases, can be quite counterintuitive, as we analyze in Appendix A. The case study of Appendix A shows that these methods may end up interpolating different primary color components in different directions, contradicting their aim to trace the edges and violating a basic physical constraint that the primary color channels should agree in gradient in natural scenes. This inconsistency in primary color interpolation often causes objectionable color noises. Having found the root cause of many color interpolation artifacts, we focus in this section on how to maintain primary consistency in color interpolation.

Given a pixel in the mosaic, we interpolate each of the missing color components twice, in horizontal and vertical directions separately. Unlike existing color demosaicking algorithms, we do not decide on the gradient direction at the time of color interpolation due to lack of information. The decision between the two interpolations (or weighting of the two) for the pixel is delayed till the results of both interpolations are available for all the missing color components in a local window. This delayed decision process is the subject of Section III, where the results of this section will be integrated into a soft decision process to form the so-called PCSD framework of color demosaic.

Denote by $({}^hr, {}^hg, {}^hb)$ and $({}^vr, {}^vg, {}^vb)$ the interpolated colors in horizontal and vertical directions. There are eight possible combinations of estimating one of the two missing primary color components in four different mosaic sample contexts (we need to estimate two other missing components at the center in each case)

$$\begin{array}{cccccccccccc} R & G & R & B & G & B & G & R & G & G & B & G \\ G & B & G & G & R & G & B & G & B & R & G & R \\ R & G & R & B & G & B & G & R & G & G & B & G. \end{array}$$

Using the symmetry, we can reduce these eight combinations to three cases and will treat each of them in the following three subsections. We remind the reader that our PCSD color demosaicking approach needs to process these three cases in the order as they are presented below.

A. Interpolation of Missing G Values

First, consider the case of interpolating the missing G value at the location of an R sampling position in the Bayer pattern as illustrated in Fig. 1.

The missing G value will be interpolated tentatively in both horizontal and vertical directions

$$ {}^hg_c = \frac{1}{2}(G_w + G_e) + \frac{1}{4}(R_c - R_{ww} + R_c - R_{ee}) \quad (1)$$

$$ {}^vg_c = \frac{1}{2}(G_n + G_s) + \frac{1}{4}(R_c - R_{nn} + R_c - R_{ss}). \quad (2)$$

As a convention of this paper, capital letters refer to original primary color values in the Bayer sampling scheme, small letters refer to reconstructed primary color values obtained by color demosaicking, and the subscripts denote the relative geographic locations as in Fig. 1. An interpretation of (1) is

$$\begin{aligned} g_{\text{Left}} - G_w &\approx (R_c - R_{ww})/2 \\ g_{\text{Right}} - G_e &\approx (R_c - R_{ee})/2 \\ {}^hg_c &= (g_{\text{Left}} + g_{\text{Right}})/2 \end{aligned}$$

where $g_{\text{Left}}(g_{\text{Right}})$ is the estimate of G for the current position using its west (east) neighbors. Clearly, the assumption used in (1) is that the horizontal gradients in red and green channels are approximately the same. The same assumption applies to (2) in a symmetry between horizontal and vertical directions. The advantage of using the adjacent red samples in the interpolation direction to interpolate the missing green value is that they can factor in the second-order term in the green channel. Note that the interpolation filter of (1) and (2) is the same as the second-order Laplacian correction filter proposed by Adams and Hamilton [1], [9]. The only difference is in that we interpolate in both horizontal and vertical directions and choose one of the two later in a larger context (a soft delayed decision), as will be explained in Section III, whereas the algorithm of Hamilton [9] makes a hard decision on the interpolation direction on a pixel-by-pixel basis.

The interpolation of missing green values at the blue sampling positions of the Bayer pattern is symmetric to the case considered above. One only needs to replace R values of (1) and (2) by corresponding B values.

After all the missing green values are tentatively interpolated in both horizontal and vertical directions, we proceed to interpolate the missing red and blue values. The reason for interpolating the missing green values before other two primary colors is two fold. First, green interpolation tends to be more robust because the sampling frequency of the green channel is twice as high as that of the other two primary color channels. Second, once the missing green values are reconstructed, we have a full-resolution green image that can greatly aid the interpolation of missing red and blue values, as we will see in the discussions to follow immediately.

B. Interpolation of Missing R/B Values at G Sampling Positions

Next, we proceed to interpolate the missing R and B values at a G sampling position. For concreteness and without loss of generality, let us examine a subcase.

1) Subcase 1: G sampling position with horizontal R and vertical B neighbors, as illustrated below

$$R_w, {}^h g_w, {}^v g_w \qquad \begin{matrix} B_n, {}^h g_n, {}^v g_n \\ G_c \\ B_s, {}^h g_s, {}^v g_s. \end{matrix} \qquad R_e, {}^h g_e, {}^v g_e$$

Note that, by now, all four neighboring green values $({}^h g_w, {}^v g_w), ({}^h g_e, {}^v g_e), ({}^h g_n, {}^v g_n), ({}^h g_s, {}^v g_s)$ interpolated in both directions are available. Using these reconstructed green values and the original sample values, we compute

$$\begin{aligned} {}^h r_c &= G_c + \frac{1}{2}\left(R_w - {}^h g_w + R_e - {}^h g_e\right) \\ {}^v r_c &= G_c + \frac{1}{2}\left(R_w - {}^v g_w + R_e - {}^v g_e\right) \\ {}^h b_c &= G_c + \frac{1}{2}\left(B_n - {}^h g_n + B_s - {}^h g_s\right) \\ {}^v b_c &= G_c + \frac{1}{2}\left(B_n - {}^v g_n + B_s - {}^v g_s\right). \end{aligned} \tag{3}$$

Since blue color is not sampled at all in the current row and red samples are completely missing in the current column, maintaining primary consistency is difficult when estimating ${}^v r_c$ and ${}^h b_c$. The vertical R interpolation ${}^v r_c$ has to use red samples of the horizontal neighbors R_w, R_e and ${}^v r_c = G_c + (1/2)(R_w - {}^v g_w + R_e - {}^v g_e)$, which is in conflict with the underlying assumption of vertical structure. The best one can do here is to fully utilize available vertical information of the neighboring columns. The green estimates ${}^v g_w$ and ${}^v g_e$ associated with R_w and R_e are used to estimate ${}^v r_c$. It is important to realize that ${}^v g_w$ and ${}^v g_e$ are estimates under the hypothesis of vertical structure. The influence of the vertical structure to the missing red value in the current column is factored in by assuming that the difference image between the red and green channels is reasonably smooth in the small locality. Namely, ${}^v r_c - G_c \approx (1/2)(R_w - {}^v g_w + R_e - {}^v g_e)$. The use of ${}^v g_w$ and ${}^v g_e$ in our estimate of ${}^v r_c$ is to respect primary consistency the best way we know in this case. This also explains why we need to first estimate all the missing green values under the hypotheses of horizontal and vertical sample structures separately. Here again, our interpolation filters in (3) would appear to be very similar to those used by Hamilton [9] and Adams [1]. However, t there is one critical difference. The methods of [9] and [1] do not guarantee that the green estimates used to interpolate the missing red or blue sample are generated by the second-order Laplacian filter in the same direction. For instance, the interpolation of r_c can use ${}^v g_w$ as the estimate of g_w but ${}^h g_e$ as the estimate of g_e, because g_w and g_e are estimated individually in [9] and [1]. This individual decision making process can violate primary consistency and cause severe artifacts as we will show in detail in Appendix B. The primary consistency can be preserved better in our soft-decision framework to be developed in Section III. At that point, the reader will appreciate why we maintain two sets of estimates, one for each hypothesis of edge direction.

2) Subcase 2: Consider the following mosaic configuration of G sampling position with horizontal B and vertical R neighbors:

$$B_w, {}^h g_w, {}^v g_w \qquad \begin{matrix} R_n, {}^h g_n, {}^v g_n \\ G_c \\ R_s, {}^h g_s, {}^v g_s. \end{matrix} \qquad B_e, {}^h g_e, {}^v g_e$$

The estimates of missing R and B for G sampling position with horizontal B and vertical R neighbors can be derived symmetrically to Subcase 1 under the same rationale. Namely

$$\begin{aligned} {}^h b_c &= G_c + \frac{1}{2}\left(B_w - {}^h g_w + B_e - {}^h g_e\right) \\ {}^v b_c &= G_c + \frac{1}{2}\left(B_w - {}^v g_w + B_e - {}^v g_e\right) \\ {}^h r_c &= G_c + \frac{1}{2}\left(R_n - {}^h g_n + R_s - {}^h g_s\right) \\ {}^v r_c &= G_c + \frac{1}{2}\left(R_n - {}^v g_n + R_s - {}^v g_s\right). \end{aligned} \tag{4}$$

C. Interpolation of Missing R/B Values at B/R Sampling Positions

The most difficult task for color demosaicking of the Bayer pattern is to estimate the missing blue (red) value at a red (blue) sampling position. This is because the blue (red) color is not sampled at all in both the current row and current column. The missing blue (red) value has to be inferred from the samples at the four corners or beyond. Specifically, consider the following mosaic configuration of missing blue value at the red sampling position:

$$\begin{matrix} B_{nw}, {}^h g_{nw}, {}^v g_{nw} & & B_{ne}, {}^h g_{ne}, {}^v g_{ne} \\ & R_c, {}^h g_c, {}^v g_c & \\ B_{sw}, {}^h g_{sw}, {}^v g_{sw} & & B_{se}, {}^h g_{se}, {}^v g_{se}. \end{matrix}$$

In this case, on the same line of reasoning as in Subcase 1, the primary-consistent estimates are

$$\begin{aligned} {}^h b_c &= {}^h g_c + \frac{1}{4} \sum_{p \in (nw,ne,sw,se)} \left(B_p - {}^h g_p\right) \\ {}^v b_c &= {}^v g_c + \frac{1}{4} \sum_{p \in (nw,ne,sw,se)} \left(B_p - {}^v g_p\right). \end{aligned} \tag{5}$$

Again, note the association of ${}^h\beta_i = {}^hb_i - {}^hg_i$ with ${}^h\gamma_i = {}^hr_i - {}^hg_i$ and the association of ${}^hg$ with ${}^hb$ in the estimation formula for primary consistency.

Estimation of missing red value at the blue sampling position is symmetric. Namely

$$\begin{aligned} {}^hr_c &= {}^hg_c + \frac{1}{4}\left(R_{nw} - {}^hg_{nw} + R_{ne} - {}^hg_{ne} \right. \\ &\quad \left. + R_{sw} - {}^hg_{sw} + R_{se} - {}^hg_{se}\right) \\ {}^vr_c &= {}^vg_c + \frac{1}{4}\left(R_{nw} - {}^vg_{nw} + R_{ne} - {}^vg_{ne} \right. \\ &\quad \left. + R_{sw} - {}^vg_{sw} + R_{se} - {}^vg_{se}\right). \end{aligned} \tag{6}$$

III. Soft Decision on Estimates

The second defining characteristic of the proposed PCSD color demosaicking approach is a novel framework of estimation via soft decision. As presented in the previous section, two sets of color estimates $({}^hr, {}^hg, {}^hb)$ and $({}^vr, {}^vg, {}^vb)$ are made for each pixel based on two different hypotheses of horizontal and vertical image structures. In either estimated color, one of the three primaries is the true sample value and the other two are estimated. Although the two hypotheses are mutually conflicting, under each hypothesis color interpolation is performed to maintain primary consistency. The decision on which interpolation result to use is delayed until each of the hypotheses can be better corroborated by sample statistics of all three estimated color channels at full resolution in a sufficiently large window centered at the pixel in question.

Specifically, define the primary differences under horizontal and vertical hypotheses at position i to be

$$\begin{aligned} {}^h\gamma_i &= {}^hr_i - {}^hg_i, \quad {}^h\beta_i = {}^hb_i - {}^hg_i \\ {}^v\gamma_i &= {}^vr_i - {}^vg_i, \quad {}^v\beta_i = {}^vb_i - {}^vg_i. \end{aligned} \tag{7}$$

In order to select between the horizontal and vertical estimates, the primary differences of horizontally estimated colors in a 3×3 window

$$\begin{matrix} \left({}^h\gamma_{nw}, {}^h\beta_{nw}\right) & \left({}^h\gamma_{n}, {}^h\beta_{n}\right) & \left({}^h\gamma_{ne}, {}^h\beta_{ne}\right) \\ \left({}^h\gamma_{w}, {}^h\beta_{w}\right) & \left({}^h\gamma_{c}, {}^h\beta_{c}\right) & \left({}^h\gamma_{e}, {}^h\beta_{e}\right) \\ \left({}^h\gamma_{sw}, {}^h\beta_{sw}\right) & \left({}^h\gamma_{s}, {}^h\beta_{s}\right) & \left({}^h\gamma_{se}, {}^h\beta_{se}\right) \end{matrix} \tag{8}$$

are used to verify the horizontal hypothesis in the window. If the hypothesis of horizontal edge is correct, then the horizontal gradients in the difference image between the estimated color channels in the window centered at the pixel in question should be small. In order to verify this, we further define the horizontal and vertical gradients of the horizontally estimated colors by

$${}_h\Delta_h = \sum_{\substack{(nw,n),(ne,n),(nw,ne) \\ (p,q)\in\{(w,c),(e,c),(w,e), \\ (sw,s),(se,s),(sw,se)\}}} \times \left\| \left({}^h\gamma_p, {}^h\beta_p\right) - \left({}^h\gamma_q, {}^h\beta_q\right) \right\|_1 \tag{9}$$

and

$${}_v\Delta_h = \mathrm{Min}\left\{ \begin{aligned} &\sum_{(p,q)\in\{nw,w),(n,c),(ne,e)\}} \left\| \left({}^h\gamma_p, {}^h\beta_p\right) \right. \\ &\quad \left. - \left({}^h\gamma_q, {}^h\beta_q\right) \right\|_1 \\ &\sum_{(p,q)\in\{sw,w),(s,c),(se,e)\}} \left\| \left({}^h\gamma_p, {}^h\beta_p\right) - \left({}^h\gamma_q, {}^h\beta_q\right) \right\|_1 \end{aligned} \right\}. \tag{10}$$

Similarly, in order to verify the hypothesis of vertical edge or structure using the vertical gradients of the difference image between the estimated color channels in the 3×3 window, we define

$${}_v\Delta_v = \sum_{\substack{(nw,w),(n,c),(ne,e) \\ (p,q)\in\{(sw,w),(s,c),(se,e), \\ (nw,sw),(n,s),(ne,se)\}}} \times \left\| \left({}^v\gamma_p, {}^v\beta_p\right) - \left({}^v\gamma_q, {}^v\beta_q\right) \right\|_1 \tag{11}$$

$${}_h\Delta_v = \mathrm{Min}\left\{ \begin{aligned} &\sum_{\substack{(nw,n) \\ (p,q)\in\{(w,c), \\ (sw,s)\}}} \left\| \left({}^v\gamma_p, {}^v\beta_p\right) - \left({}^v\gamma_q, {}^v\beta_q\right) \right\|_1 \\ &\sum_{\substack{(ne,n) \\ (p,q)\in\{(e,c), \\ (se,s)\}}} \left\| \left({}^v\gamma_p, {}^v\beta_p\right) - \left({}^v\gamma_q, {}^v\beta_q\right) \right\|_1 \end{aligned} \right\}. \tag{12}$$

In choosing between the horizontal and vertical estimates, the gradients ${}_h\Delta_h$ and ${}_v\Delta_v$ play a major role in making the decision, whereas ${}_v\Delta_h$ and ${}_h\Delta_v$ are secondary and useful to break the tie if ${}_h\Delta_h$ and ${}_v\Delta_v$ are too close to discriminate. Now, the problem of testing interpolation hypotheses can be treated as one of optimal statistical decision. Let the decision whether $({}^hr, {}^hg, {}^hb)$ or $({}^vr, {}^vg, {}^vb)$ is a better estimate of the concerned pixel be a binary random variable X. The soft decision for color demosaicking is based on the posterior probability $P(X|{}_h\Delta_h, {}_v\Delta_h, {}_v\Delta_v, {}_h\Delta_v)$. This posterior probability can be estimated from a large suitable training set. One can apply the classic maximum a posterior probability (MAP) techniques to solve the problem. Minimum-risk Bayesian classifier [7] and Fisher's linear discriminant technique [6] also proved to be effective in our experiments. We describe the latter technique below in the context of color demosaic.

We consider $\mathbf{z} = ({}_h\Delta_h, {}_v\Delta_h, {}_v\Delta_v, {}_h\Delta_v)$ to be a vector of features that the binary random variable X exhibits, where $X = 1$ if $({}^hr, {}^hg, {}^hb)$ is a better estimate than $({}^vr, {}^vg, {}^vb)$ and $X = 0$ otherwise. We use a suitable training set $\mathbf{Z} = \{\mathbf{z}_1, \mathbf{z}_2, \ldots, \mathbf{z}_k\}$

representing the statistics of the CCD camera data to optimize the binary decision X. The value of X partitions the set $\mathbf{Z}$ into two subsets $\mathbf{Z}_0$ and $\mathbf{Z}_1$. Set $\mathbf{Z}_0(\mathbf{Z}_1)$ consists of all the training feature vectors associated with $X = 0(X = 1)$. The problem of optimal soft decision for color demosaicking is then converted to one of maximum separation of the two sets $\mathbf{Z}_0$ and $\mathbf{Z}_1$ in the feature space of $\mathbf{z}$ by a classifier. This can be done by Fisher's linear discriminant [6], which aims to separate $\mathbf{Z}_0$ and $\mathbf{Z}_1$ by a hyperplane. The hyperplane is set perpendicular to the direction in which $\mathbf{Z}_0$ and $\mathbf{Z}_1$ have the maximum separation. Specifically, we want to find the projection direction $\mathbf{a}$

$$\mathbf{a} = \arg\max_{\mathbf{x}} \frac{(\mu_0(\mathbf{x}) - \mu_1(\mathbf{x}))^2}{\sigma_0^2(\mathbf{x}) + \sigma_1^2(\mathbf{x})} \tag{13}$$

where

$$\mu_i(\mathbf{x}) = E\{\mathbf{x}^T\mathbf{z} \,|\, \mathbf{z} \in \mathbf{Z}_i\}, \quad i = 0, 1 \tag{14}$$

and

$$\sigma_i^2(\mathbf{x}) = E\{(\mathbf{x}^T\mathbf{z} - \mu_i(\mathbf{x}))^2 \,|\, \mathbf{z} \in \mathbf{Z}_i\}, \quad i = 0, 1. \tag{15}$$

The solution of (13) is well known in multivariate analysis

$$\mathbf{a} = \mathbf{S}^{-1}(\mathbf{m}_0 - \mathbf{m}_1) \tag{16}$$

where

$$\mathbf{m}_i = \frac{1}{|\mathbf{Z}_i|} \sum_{\mathbf{z} \in \mathbf{Z}_i} \mathbf{z} \quad i = 0, 1 \tag{17}$$

and

$$\mathbf{S} = \frac{1}{|\mathbf{z}_0|} \sum_{\mathbf{z} \in \mathbf{Z}_0} (\mathbf{z} - \mathbf{m}_0)(\mathbf{z} - \mathbf{m}_0)^T + \frac{1}{|\mathbf{z}_1|} \sum_{\mathbf{z} \in \mathbf{Z}_1} (\mathbf{z} - \mathbf{m}_1)(\mathbf{z} - \mathbf{m}_1)^T. \tag{18}$$

Once the maximum separation direction $\mathbf{a}$ is determined, the optimal estimate can be made by the following linear function

$$\begin{aligned} &\text{if } \mathbf{z}\mathbf{a}^T < \xi \\ &\quad X = 0 \;/* \text{ choose } ({}^v r, {}^v g, {}^v b) */ \\ &\text{else} \\ &\quad X = 1 \;/* \text{ choose } ({}^h r, {}^h g, {}^h b) */ \end{aligned} \tag{19}$$

where the threshold value ξ can be optimally chosen by a linear search using a suitable training set. The optimization criterion can be to minimize the mean-square estimation error or to minimize the number of misclassifications. We found empirically that the latter criterion produces slightly better visual quality. This observation can be easily explained because the reviewers prefer a reconstructed image with as few wrongly interpolated pixels as possible to one of slightly higher PSNR.

We implemented the Fisher's linear discriminant and found that the optimal projection direction is given by

$$\hat{\mathbf{a}} = (-0.62, -0.35, +0.62, +0.35)$$

for a very large training set of 36 test images. Interestingly enough, even without training or optimization, we found empirically that the parameters $\mathbf{a} = (-1, 0, 1, 0)$ and $\xi = 0$ worked quite well on natural color images. The following examples (Fig. 7) demonstrate the difference in image quality between the optimized Fisher discriminant and the simple fast linear classifier $\mathbf{a} = (-1, 0, 1, 0)$.

To conclude this section, we would like to emphasize that the proposed PCSD methodology of PCSD color demosaicking represents a general framework. It can be realized by other statistical inference techniques. The above development only showed how the problem can be solved as one of optimal decision or minimum-risk classification. The problem can also be treated as one of data fusion so that the two or more estimates under different hypotheses can be weighted to minimize the estimation error. If color demosaicking is treated as a binary decision problem as proposed earlier, we essentially choose between one of the two one-dimensional (1-D) (horizontal or vertical) interpolation filters. If the interpolation direction is chosen correctly, the 1-D filtering is optimal in the presence of edges. In smooth color areas, the 1-D filtering also works satisfactorily because the signal is smooth in either direction. However, two-dimensional (2-D) filtering should be clearly superior, at least in terms of PSNR measure, for signals that are isotropic and smooth. Therefore, optimal data fusion is a more general and robust approach in the soft-decision color demosaicking framework. The research on this approach is under way. Finally, the features on which the statistical inference is based are very important to the performance of soft-decision color demosaic, too. The feature vector $({}_h\Delta_h, {}_v\Delta_h, {}_v\Delta_v, {}_h\Delta_v)$ proposed here is by no means the only choice. It can be easily replaced by any other feature vectors, if one can find a set of more revealing and discriminating features.

IV. Experimental Results

To evaluate the performance of the new PCSD color demosaicking methodology, we compared the new method to the best in the literature [1], [4], and [9]. Our experiments were controlled to calibrate the impact of the primary-consistent interpolation and soft-decision estimates only. No pre- and post-processing is used. When interpolating the missing green samples, we use the same five-tap second-order Laplacian correction filter as in [9], which was observed by many authors including us to be one of the best practical demosaicking filters. Like in [9], we assumed the smoothness of the difference image between different color channels, as being evident in (1) and (2). The only difference is in that we chose ${}^h g$ and ${}^v g$ differently in order to ensure primary consistency and the interpolation is done separately under two different hypotheses

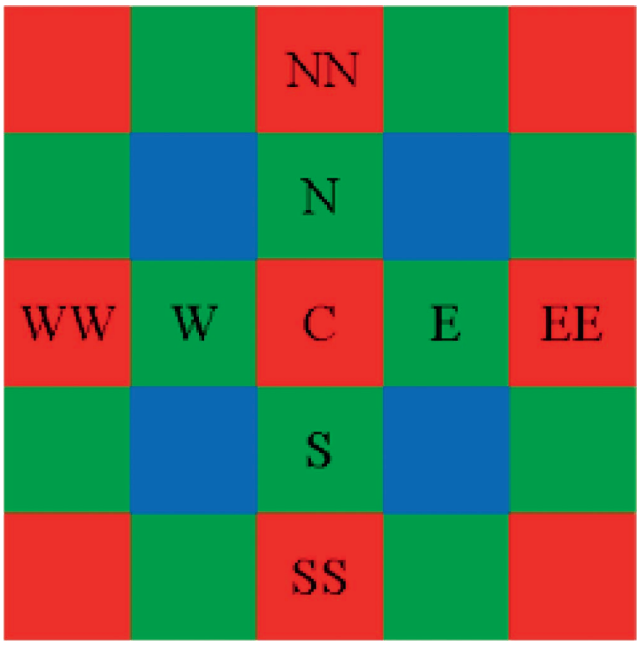

Fig. 1. Bayer pattern.

Fig. 2. Images used in experiments. They are referred to as Bikes, Ribbon, Water, Fence, Sail, and Barb in the text, enumerated from left to right and top to bottom.

on edge direction. After missing green samples are estimated, we use the simplest bilinear color difference interpolation to reconstruct the missing red and blue samples. Under these experimental conditions, one can be sure that any performance differences between Hamilton's algorithm and the PCSD algorithm, either by subjective or objective measures, are solely the effects of primary-consistent color interpolation and soft-decision estimation.

Our comparative performance evaluation of different color demosaicking algorithms [1], [4], and [9] was carried out on a large set of natural color images of different resolutions. Some of our test images are shown in Fig. 2. These images have three full-resolution red, green, and blue color channels. The color filter array (CFA) is simulated by sampling the three color channels according to Bayer pattern. No antialiasing preprocessing is performed in the subsampling. The existing demosaicking algorithms chosen in the study group are among the best so far in the literature. Tables I, II, and III tabulate the PSNR results (in decibles) of different color demosaicking algorithms, each of the primary colors green, red, and blue, respectively. As one can see from the tables, the PCSD algorithm outperforms existing ones by significant margins. The difference ranges from 1.6 to 4.6 dB on an average of six test images. In some instances, the gap can be as large as 7.9 dB. In Appendix B, we use the test image of picket fence in a case study to explain why such a large performance gap exists between the PCSD approach and others.

To assess the visual quality of different demosaicking algorithms, in Figs. 3–6, we present the original and reconstructed color images by different algorithms in some areas of four test images Fence, Barb, Water, and Ribbon. These images, while being common scenes in photography, contain some most difficult high frequency features such as picket fences (Fig. 3), fine fiber patterns (Figs. 4 and 5) and water texture (Fig. 6) that can challenge digital cameras, or so-called "heartburn" cases identified by [2]. The superior image quality of the PCSD algorithm over others is clearly demonstrated by the color plates of Figs. 3–6.

With the validity and effectiveness of the PCSD color demosaicking approach established, we also experimented with post-processing filtering to further improve the demosaicking results, in particular, in terms of objective error measure. Recently, Gunturk *et al.* published a color demosaicking technique, called alternating projections [8], to improve Hamilton–Adams' method. It is essentially an iterative low-pass filtering scheme under the assumption of smooth difference image between the color channels. Gunturk *et al.* used Hamilton–Adams' method to get initial estimates of missing green samples. The interpolated green samples at the red (blue) locations are used to form a down-sampled version of the green channel. The original mosaic samples of the red (blue) channel form down-sampled red (blue) channel to correspond to the down-sampled green channel. These down-sampled green and red (blue) channels are then wavelet transformed into LL, HL, LH, and HH subbands. The current green estimates at red (blue) locations are updated by replacing green channel's high frequency (LH, HL, HH) subbands with those of the red (blue) channel. Actually, the above procedure is equivalent to the filtering of the down sampled color difference images $\gamma = \mathbf{R} - \mathbf{g}$ and $\beta = \mathbf{B} - \mathbf{g}$ by a 5×5 2-D low-pass filter $\mathbf{F}$, where

$$\mathbf{F} = \mathbf{f}\mathbf{f}^T, \quad \mathbf{f} = \left(-\frac{1}{8}, \frac{1}{4}, \frac{3}{4}, \frac{1}{4}, -\frac{1}{8}\right).$$

The resulting low-pass filtered images $\hat{\gamma}$ and $\hat{\beta}$ are then used to update green color estimations as $\hat{\mathbf{g}} = \mathbf{R} - \hat{\gamma}$ and $\hat{\mathbf{g}} = \mathbf{B} - \hat{\beta}$ at red and blue locations. After the missing green samples are interpolated, iterative wavelet transform and projection operations are used to finish red and blue interpolations (see [8] for details). The idea of [8] is to make the high frequency energy of reconstructed color difference images below certain threshold without changing original mosaic sample values. Gunturk *et al.* reported higher PSNR values than those of other algorithms.

Adaptive post filtering can be integrated into the proposed PCSD demosaicking framework. After tentative color interpolations performed separately under hypotheses of horizontal and vertical gradients, but before soft decision, we examine the four full-resolution color difference images

$$^h\gamma = {}^h\mathbf{r} - {}^h\mathbf{g}, \quad {}^v\gamma = {}^v\mathbf{r} - {}^v\mathbf{g}, \quad {}^h\beta = {}^h\mathbf{b} - {}^h\mathbf{g}$$
$$^v\beta = {}^v\mathbf{b} - {}^v\mathbf{g}.$$

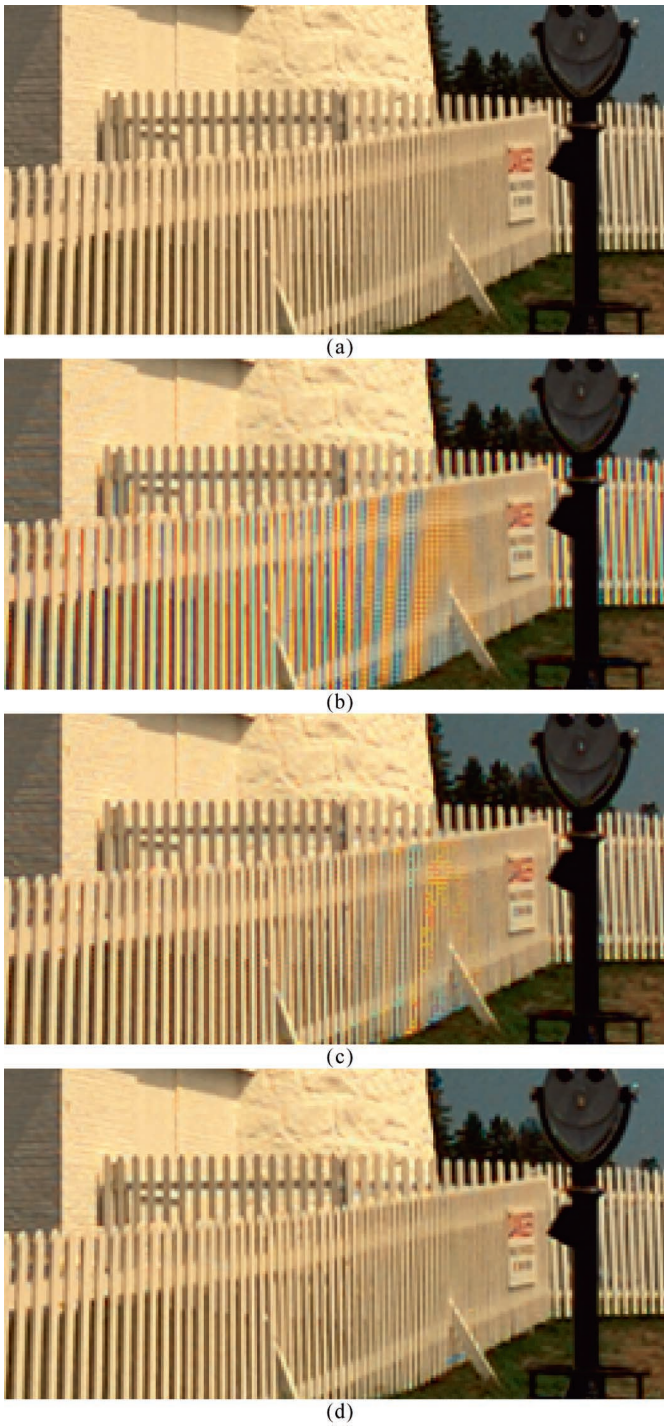

Fig. 3. Color reproduction comparison of different color demosaicking algorithms. (a) Part of the original image fence. (b) Algorithm of [4]. (c) Algorithm of [9]. (d) PCSD.

Fig. 4. Color reproduction comparison of different color demosaicking algorithms. (a) Part of the original image barb. (b) Algorithm of [4]. (c) Algorithm of [9]. (d) PCSD.

Instead of using a separable 2-D low-pass filter as in [8] without edge adaptability, we can employ a directional filter. Specifically, we can filter ${}^{h}\gamma$ and ${}^{h}\beta$ along horizontal direction while filter ${}^{v}\gamma$ and ${}^{v}\beta$ along vertical direction. A simple five-tap average filter $\mathbf{f} = (1/5, 1/5, 1/5, 1/5, 1/5)$ was found to perform well.

By low-pass filtering of interpolation results under different hypotheses before soft decision (hypothesis verification), our reconstructed green images have on average 2.4-dB higher PSNR than [8] (see Table IV). This improvement is significant in terms of subjective quality because the green channel in the Bayer pattern contains much of the spatial detail. Moreover, the average PSNR value of blue images (which were reconstructed by simple bilinear interpolation of the β signal after all green samples have been determined) is also 1.2-dB higher than the results reported in [8], even though the latter required

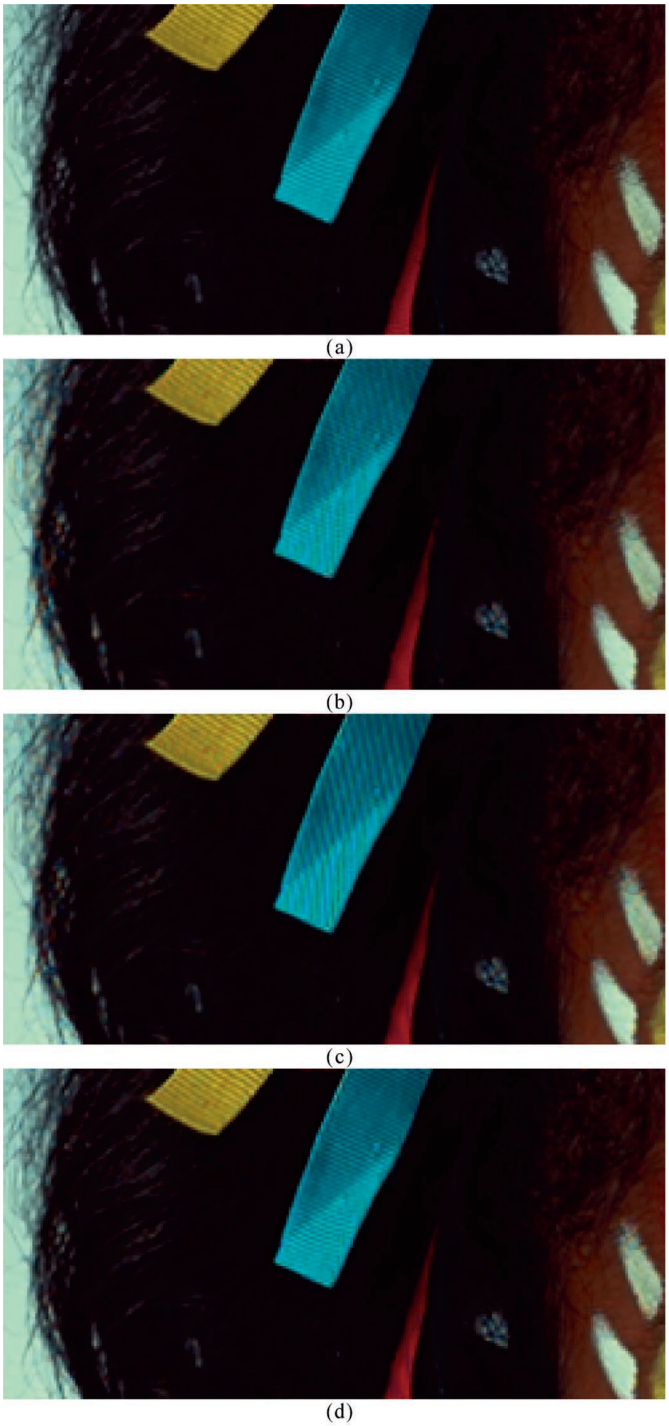

Fig. 5. Color reproduction comparison of different color demosaicking algorithms. (a) Part of the original image ribbon. (b) Algorithm of [4]. (c) Algorithm of [9]. (d) PCSD.

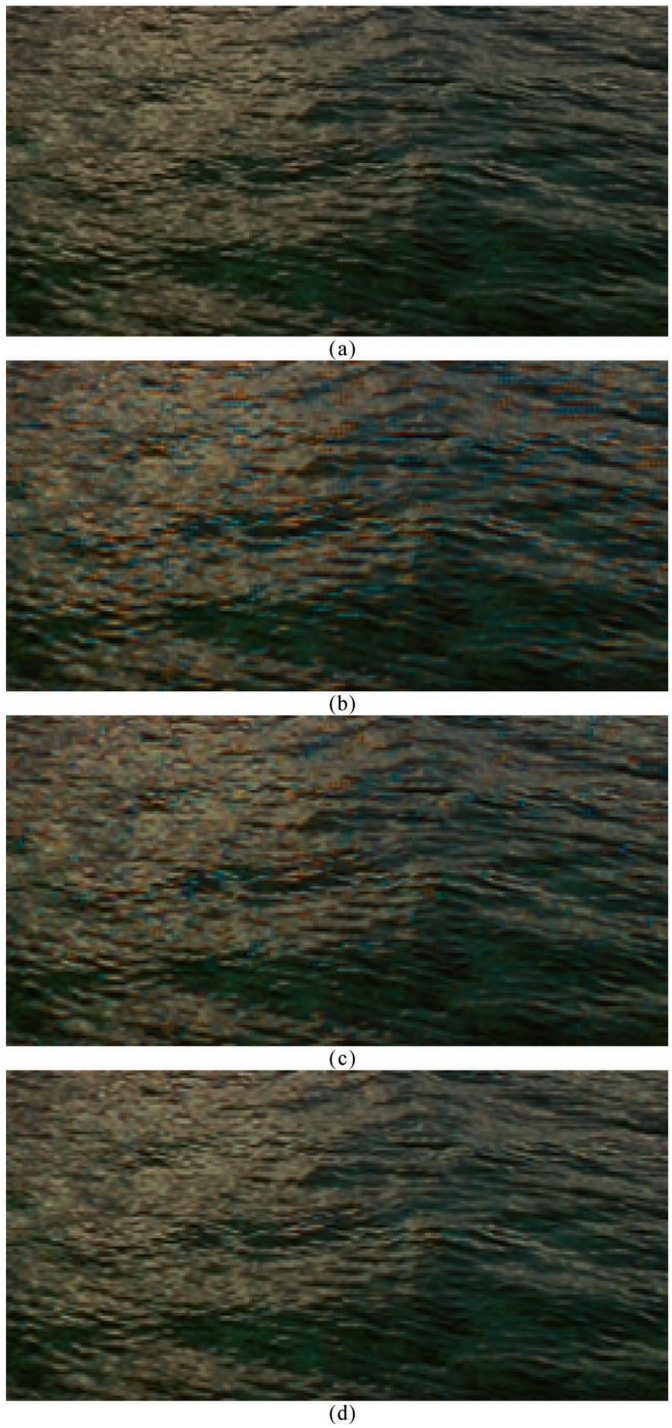

Fig. 6. Color reproduction comparison of different color demosaicking algorithms. (a) Part of the original image water. (b) Algorithm of [4]. (c) Algorithm of [9]. (d) PCSD.

several (about 8) iterations of wavelet transform and alternating projections.

V. Conclusion

In this paper, we proposed a new PCSD framework of color demosaicking techniques and presented a PCSD-based color demosaicking method using the second-order Laplacian correction filter and Fisher linear discriminant. Our analysis and experimental results show that the PCSD demosaicking method can eliminate or greatly alleviate many types of objectionable color artifacts of existing color demosaicking methods. We believe that further improvement in fidelity of demosaiced color images captured by digital cameras is possible within the new PCSD framework, with discovery of better interpolation filters and statistical inference techniques.

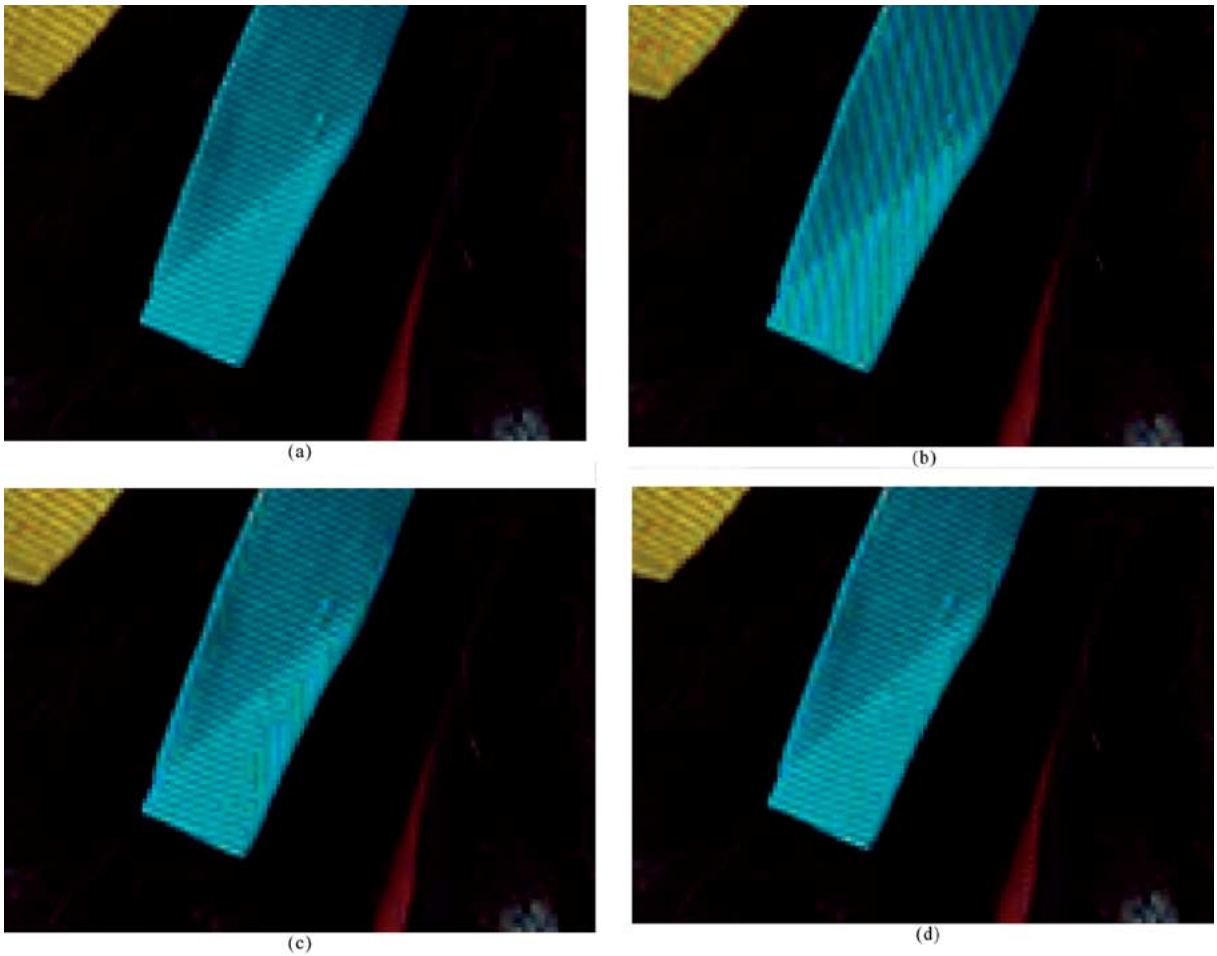

Fig. 7. Color reproduction comparison of different color demosaicking algorithms. (a) Part of the original image ribbon. (b) Algorithm of [9]. (c) PCSD [no training: $\mathrm{a} = (-1, 0, 1, 0)$]. (d) PCSD [Fisher discriminant: $\hat{\mathbf{a}} = (-0.62, -0.35, +0.62, +0.35)$].

APPENDIX

A. Case Study of Primary Inconsistency in Color Interpolation

In this Appendix, we expose the problem of primary inconsistent color interpolation and its adverse effects to the image quality. For concreteness, we choose the color demosaicking algorithm of [4] to exemplify the problem. This algorithm is chosen because it went to a great length to interpolate missing color samples along estimated edge directions/trajectories. However, it does not ensure that different primary colors are interpolated consistently in the same direction/trajectory. This oversight makes directional color interpolation counterproductive in some cases as we will show below.

The algorithm of [4] interpolates a missing color component by weighting some of the eight neighboring samples of the concerned pixel based on directional gradients.

For instance, at a red position (Fig. 8), the estimates of the primary colors for the north location are

$$r_n = \frac{1}{2}(R_c + R_{nn}), \quad g_n = G_n, \quad b_n = \frac{1}{2}(B_{nw} + B_{ne}). \tag{20}$$

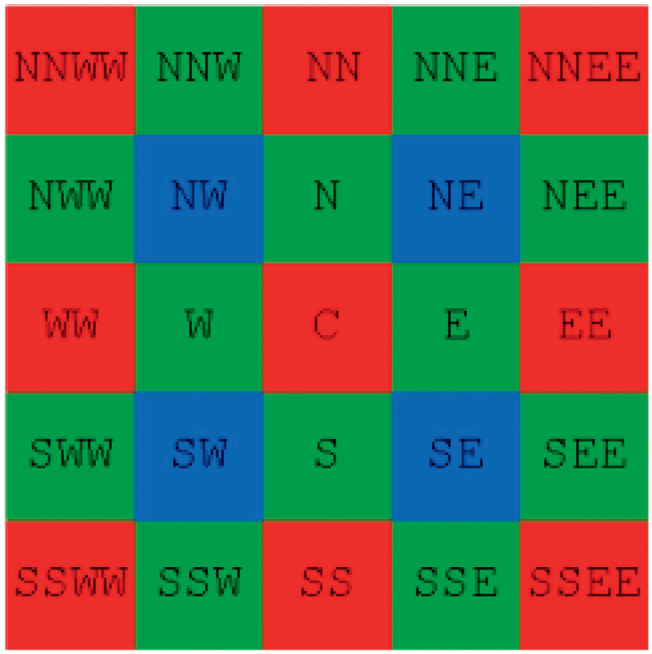

Fig. 8. Interpolate G and B for R position.

TABLE I
GREEN CHANNEL PSNR (IN DECIBELS) COMPARISON OF DIFFERENT METHODS

Image	Algorithm[9]	Algorithm[1]	Algorithm[4]	PCSD
Bikes	35.92	34.17	35.62	37.50
Ribbon	39.36	38.87	40.64	41.07
Water	39.67	38.8	40.68	42.71
Fence	38.24	37.26	38.54	39.63
Sail	37.05	36.27	37.63	38.35
Barb	33.24	33.22	34.56	38.07
Ave.	37.25	36.43	37.95	39.56

TABLE II
RED CHANNEL PSNR (IN DECIBELS) COMPARISON OF DIFFERENT METHODS

Image	Algorithm[9]	Algorithm[1]	Algorithm[4]	PCSD
Bikes	31.80	33.01	32.40	35.63
Ribbon	34.83	35.33	34.77	36.27
Water	35.87	37.38	34.63	41.17
Fence	33.31	35.79	29.63	37.24
Sail	33.20	34.63	33.91	36.01
Barb	29.68	30.63	29.25	33.89
Ave.	33.12	34.46	32.43	36.70

TABLE III
BLUE CHANNEL PSNR (IN DECIBELS) COMPARISON OF DIFFERENT METHODS

Image	Algorithm[9]	Algorithm[1]	Algorithm[4]	PCSD
Bikes	31.78	32.75	32.01	35.04
Ribbon	35.65	37.15	34.86	38.88
Water	35.91	37.14	34.57	40.61
Fence	33.55	35.92	29.90	37.81
Sail	33.41	34.65	33.97	35.97
Barb	29.63	30.51	29.11	33.70
Ave.	33.32	34.69	32.40	37.00

Whether and how much estimate (r_n, g_n, b_n) contributes to the estimate (r_c, g_c, b_c) of the center pixel depends on gradient d_n

$$d_n = |G_n - G_s| + |R_{nn} - R_c| + \frac{1}{2}|B_{nw} - B_{sw}| + \frac{1}{2}|B_{ne} - B_{se}| + \frac{1}{2}|G_{nnw} - G_w| + \frac{1}{2}|G_{nne} - G_e|.$$

Note that in (20), estimate r_n is obtained via an interpolation in vertical direction but estimate b_n in horizontal direction. This is clearly a case of primary inconsistency, because the red and blue interpolations are performed in perpendicular directions. Suppose that there is a vertical edge, and d_n is relatively small so that (r_n, g_n, b_n) gets selected. However, because b_n is not estimated in vertical direction, the algorithm of [4] can cause severe color artifacts even for simple vertical edges. Symmetrically, other cases of primary inconsistency also exist.

To see a case in point, let us examine the following 2-D mosaic sample data:

$$\begin{array}{ccccc} R_{166} & G_{206} & R_{242} & G_{106} & R_{103} \\ G_{142} & B_{165} & G_{224} & B_{61} & G_{87} \\ R_{156} & G_{207} & R_{242} & G_{96} & R_{106} \\ G_{143} & B_{164} & G_{219} & B_{61} & G_{83} \\ R_{164} & G_{207} & R_{244} & G_{101} & R_{109} \end{array}$$

in which R_{242} represents an original red sample of value 242 in the Bayer mosaic, and so forth. The original image has a vertical edge through the center of the window. The primary

TABLE IV
PSNR (IN DECIBELS) COMPARISON BETWEEN ALGORITHM [8] AND PCSD WITH DIRECTIONAL FILTERING

Image	Algorithm [8]			PCSD with directional filtering		
	Green	Blue	Red	Green	Blue	Red
Bikes	38.76	35.66	37.93	40.42	36.19	36.99
Ribbon	39.04	39.20	38.85	42.76	40.35	36.67
Water	43.30	40.91	42.14	45.95	42.16	43.17
Fence	40.90	38.77	40.04	42.60	40.80	39.29
Ave.	40.50	38.64	39.74	42.93	39.88	39.03

TABLE V
PRIMARY COLOR VALUES AND GRADIENTS IN EIGHT DIRECTIONS ESTIMATED BY THE ALGORITHM OF [4]

	n	e	s	w	ne	se	sw	nw
r_p	242	174	243	199	172	175	203	204
g_p	**224**	**96**	**219**	**207**	128	124	194	194
b_p	113	61	112	164	**61**	**61**	**164**	**165**
d_p	10	486	9	379	374	372	288	291

color values and gradients (r_p, g_p, b_p, d_p) in eight directions $p \in \{n, e, s, w, ne, se, sw, nw\}$, estimated by the algorithm of [4] are tabulated in Table V. The values in bold face are original mosaic data, while others are estimates obtained by interpolation formula of [4] like (20).

In [4], the threshold for selecting gradients to be used in interpolation is

$$\begin{aligned} T &= 1.5d_{\min} + 0.5(d_{\max} - d_{\min}) \\ &= 1.5 \times 9 + 0.5 \times (486 - 9) = 252. \end{aligned}$$

Due to the vertical edge, in this case only, d_n and d_s are below T, so (r_n, g_n, b_n) and (r_s, g_s, b_s) are selected to interpolate the missing green and blue samples

$$\begin{aligned} g &= R_c + \frac{1}{2}(g_n - r_n + g_s - r_s) \\ &= 242 + \frac{1}{2}(224 - 242 + 219 - 243) = 221 \\ b &= R_c + \frac{1}{2}(b_n - r_n + b_s - r_s) \\ &= 242 + \frac{1}{2}(113 - 242 + 112 - 243) = 112. \end{aligned}$$

The original green and blue values for the red position in question are 220 and 180, respectively. A large error in blue estimation is caused by primary inconsistency. The color artifacts are rather conspicuous as in Figs. 3–6.

B. Case Study of Soft Decision

In the presence of high–frequency features, a key to adaptive color demosaicking is the estimation of edge direction or trajectory before interpolating missing color components accordingly. The estimation is far more difficult and less robust than edge detection in conventional image processing due to subsampling of color channels by CCD sensors. This is because the underlying intensity gradients are necessarily estimated based on incomplete information. The following example shows how an interpolation result can contradict the very assumption under which the interpolation is made, and how the problem can be rectified by the soft decision of the PCSD framework proposed by this paper.

Presented below is a block of mosaic data taken from Fig. 3(a)

$$\begin{array}{ccccc} & & R_{144} & & \\ & & G_{137} & & \\ (\mathbf{R_{180}}, {}^h g_{177}) & G_{194} & (\mathbf{R_{169}}, {}^h g_{189}, {}^v g_{147}) & G_{195} & R_{181} \\ & & G_{149} & & \\ R_{189} & G_{202} & (\mathbf{R_{178}}, {}^v g_{156}) & G_{195} & R_{181} \\ & & G_{162} & & \\ & & R_{180}. & & \end{array}$$

By convention of this paper, the capital letters represent original mosaic data, while small letters represent estimated missing sample values via demosaicking. The three sample positions identified by bold face letters $\mathbf{R_{169}}, \mathbf{R_{178}}, \mathbf{R_{180}}$ are the subjects of the following discussion. The green estimates under different edge hypotheses are also given at the three positions, with ${}^h g_{189}$ denoting the green estimate via interpolation under the assumption of horizontal edge direction, and so forth. This is the "picket fence" scenario selected by Adams *et al.* [2] as a representative of the most difficult cases for color demosaicking algorithms. The difficulty lies in the facts that the horizontal and vertical differences are too close to discriminate and that the penalty of a mistake in interpolation direction is high. It is interesting to see how Hamilton–Adams' algorithm [9], one of the best in the literature, handles this case. At red position $\mathbf{R_{169}}$, the horizontal and vertical gradients are estimated as

$$\begin{aligned} dh &= |G_{194} - G_{195}| + |R_{169} - R_{180} + R_{169} - R_{181}| = 24 \\ dv &= |G_{137} - G_{149}| + |R_{169} - R_{144} + R_{169} - R_{178}| = 28. \end{aligned}$$

Since $dh < dv$, the algorithm assumes that samples $\{\mathbf{R_{180}}, G_{194}, \mathbf{R_{169}}, G_{195}, R_{181}\}$ are on a horizontal edge and estimates the green sample for position $\mathbf{R_{169}}$ to be

$$^{h}g = \frac{1}{2}(G_{194} + G_{195}) + \frac{1}{4}(R_{169} - R_{180} + R_{169} - R_{181}) \approx 189$$

which is labeled by $^{h}g_{189}$ in the figure above. Now, consider the red position $\mathbf{R_{178}}$ below $\mathbf{R_{169}}$. At this position, the estimated horizontal and vertical gradients are

$$dh = |G_{202} - G_{195}| + |R_{178} - R_{189} + R_{178} - R_{181}| = 21$$
$$dv = |G_{149} - G_{162}| + |R_{178} - R_{169} + R_{178} - R_{180}| = 20.$$

However, here $dh > dv$, the algorithm concludes that samples $\{\mathbf{R_{169}}, G_{149}, \mathbf{R_{178}}, G_{162}, R_{180}\}$ are on a vertical edge and estimates the green sample for position $\mathbf{R_{178}}$ to be

$$^{v}g = \frac{1}{2}(G_{149} + G_{162}) + \frac{1}{4}(R_{178} - R_{169} + R_{178} - R_{180}) \approx 156.$$

The above suggests three possibilities: the pixel at position $\mathbf{R_{169}}$ is on the horizontal edge, or on the vertical edge, or at the intersection of the two perpendicular edges of similar color. The last case can be ruled out because the two edges have very different colors: At position $\mathbf{R_{169}}$ the primary difference is $R - g \approx R_{169} - {}^{h}g_{189} = -20$, whereas at position $\mathbf{R_{178}}$, we have $R - g \approx R_{178} - {}^{v}g_{157} = +22$. Now, the decision is which interpolation direction should be at position $\mathbf{R_{169}}$. This decision is prone to error if the estimation of missing primary color values is done on a pixel by pixel basis. Indeed, most of existing color demosaicking algorithms will interpolate the missing green value at position $\mathbf{R_{169}}$ horizontally, despite the fact that there is a sharp vertical edge through the pixel in question. This interpolation error causes the color artifacts as shown in Fig. 3(c).

In contrast, the probability of estimation error can be greatly reduced by soft decision. Instead of jumping to the conclusion that there is a horizontal edge through position $\mathbf{R_{169}}$, we also tentatively interpolate the missing green sample at position $\mathbf{R_{169}}$ in vertical direction

$$^{v}g = \frac{1}{2}(G_{137} + G_{149}) + \frac{1}{4}(R_{169} - R_{144} + R_{169} - R_{178}) = 147.$$

Then, we test the two conflicting hypotheses of horizontal and vertical edges by examining in which direction the primary difference signal of reconstructed color samples is smoother, i.e., selecting the direction in which the color variation is the smaller. If two neighboring pixels (r_1, g_1, b_1) and (r_2, g_2, b_2) are on an edge, then the difference values $r_1 - g_1$ and $r_2 - g_2$ tend to be approximately same. Indeed, the second-order Laplacian interpolation filter used by many authors [1], [8], [9], including us, is based on the assumption of $r_1 - g_1 \approx r_2 - g_2$. In the example above, we have $R - {}^{v}g = 22$ at position $\mathbf{R_{169}}$ and also $R - {}^{v}g = 22$ at position $\mathbf{R_{178}}$; in comparison, we have $R - {}^{h}g = -20$ at position $\mathbf{R_{169}}$ but $R - {}^{h}g = +3$ at position $\mathbf{R_{180}}$ (if the missing green sample at position $\mathbf{R_{180}}$ is interpolated horizontally by the second-order Laplacian filter, then $^{h}g = 177$). Since the primary difference signal $R - g$ is much smoother in the vertical direction than in the horizontal direction, our algorithm chooses $^{v}g = 147$ over $^{h}g = 189$ to be the estimate of the missing green value at position $\mathbf{R_{169}}$, while the true value is also 147.

REFERENCES

[1] J. E. Adams Jr. and J. F. Hamilton, "Adaptive color plane interpolation in single color electronic camera," U.S. Patent 5 506 619, Apr. 1996.

[2] J. E. Adams Jr., K. Parulski, and K. Spaulding, "Color processing in digital cameras," *IEEE Micro*, vol. 18, pp. 20–30, Nov. 1998.

[3] B. E. Bayer, "Color imaging array," U.S. Patent 3 971 065, July 1976.

[4] E. Chang, S. Cheung, and D. Y. Pan, "Color filter array recovery using a threshold-based variable number of gradients," *Proc. SPIE*, vol. 3650, pp. 36–43, 1999.

[5] T. Chen, http://www-ise.stanford.edu/tingchen/.

[6] R. A. Fisher, "The use of multiple measurements in taxonomic problems," *Ann. Eugen.*, vol. 7, pp. 179–188, 1936.

[7] K. Fukunaga, *Introduction to Statistical Pattern Recognition*, 2nd ed. Boston, MA: Academic, 1990.

[8] B. K. Gunturk, Y. Altunbasak, and R. M. Mersereau, "Color plane interpolation using alternating projections," *IEEE Trans. Image Processing*, vol. 11, pp. 997–1013, Sept. 2002.

[9] J. F. Hamilton and J. E. Adams Jr., "Adaptive color plane interpolation in single sensor color electronic camera," U.S. Patent 5 629 734, May 1997.

[10] X. Wu, W. K. Choi, and P. Bao, "Color restoration from digital camera data by pattern matching," *Proc. SPIE*, vol. 3018, pp. 12–17, 1997.

Xiaolin Wu (M'88–SM'96) received the B.Sc. degree in computer science from Wuhan University, Wuhan, China, and the Ph.D. degree in computer science from the University of Calgary, Calgary, AB, Canada, in 1982 and 1988, respectively.

He is currently a Professor in the Department of Electrical and Computer Engineering, McMaster University, Hamilton, ON, Canada, and a Research Professor of computer science at the Polytechnic University, Brooklyn, NY, and holds the NSERC-DALSA Research Chair in digital cinema. His research interests include image processing, multimedia coding and communications, data compression, and signal quantization, and he has published over 100 research papers in these fields.

Ning Zhang received the B.E. and Ph.D. degrees in electrical engineering from Tsinghua University, Beijing, China, in 1994 and 2000, respectively.

He is currently a Research Associate at McMaster University, Hamilton, ON, Canada. His research interests include data compression, image processing, multimedia communication, and digital cinema.